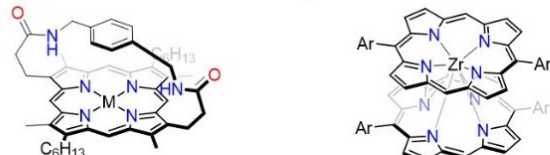


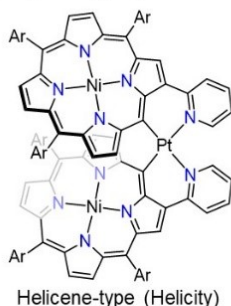
Supporting Information

(A) Variety of Pors with Intrinsic Chirality

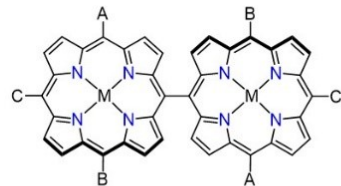


Cyclophane-type (Planar chirality)

Double-decker-type (Planar chirality)

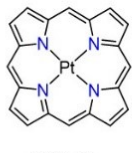


Helicene-type (Helicity)

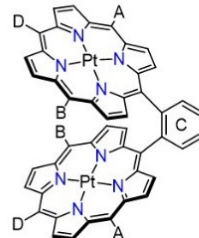


Biphenylene-type (Axial chirality)

(B) This work: Intrinsic Chirality Induction of Pt(II)-Por using ABCD-Por



Pt(II)-Por



Cofacial-type (Axial chirality $\times 2$)

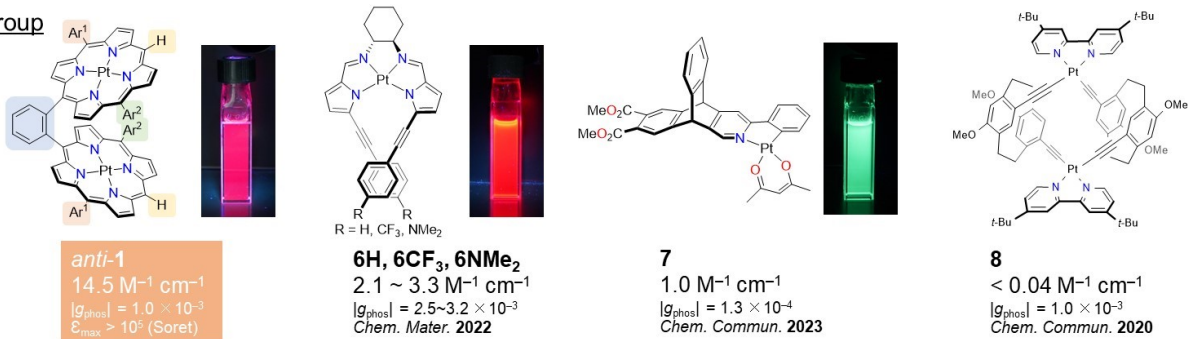
- ✓ Famous RTP emitter
- ✓ $\epsilon_{\text{Soret}} > 10^5 \text{ M}^{-1} \text{ cm}^{-1}$

- ✓ Simple synthesis
- ✓ Stable chirality without chiral inductor
- ✓ First CPP emissive Pt(II)-Por
- ✓ Bright CPP $B_{\text{CPL}} > 10^1 \text{ M}^{-1} \text{ cm}^{-1}$

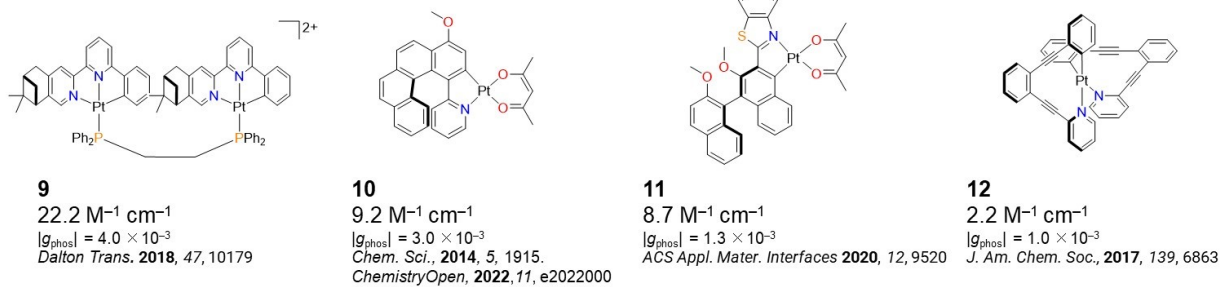
Figure S1. (A) Optically active Pors with intrinsic chirality. (B) This work: chirality induction of cofacial Pt(II)-Por dimer using ABCD substituents.

$$B_{\text{CPL}} \text{ values} = 0.5 \times \varepsilon_{\max} \times \Phi_{\text{phos}} \times g_{\text{phos}}$$

Our group



Other groups



Compound	ε_{\max} [M ⁻¹ cm ⁻¹] (λ [nm])	Φ_{phos}	$ g_{\text{phos}} $	B_{CPL} [M ⁻¹ cm ⁻¹]	reference
anti-1	4.1×10^5 (387)	0.07	1.0×10^{-3}	14.5	This work
6H (R = H)	4.9×10^4 (351)	0.05	2.6×10^{-3}	3.2	42
6CF₃ (R = CF₃)	4.3×10^4 (348)	0.04	2.5×10^{-3}	2.1	42
6NMe₂ (R = NMe₂)	5.1×10^4 (309)	0.04	3.2×10^{-3}	3.3	42
7	3.3×10^4 (252)	0.48	1.3×10^{-4}	1.0	43
8	7.6×10^4 (300)	< 0.001	1.0×10^{-3}	< 0.04	41
9	7.4×10^4 (around 240)	0.15	4.0×10^{-3}	22.2	38
10	6.1×10^4 (around 250)	0.10	3.0×10^{-3}	9.2	35–37
11	4.2×10^4 (around 310)	0.32	1.3×10^{-3}	8.7	39
12	6.4×10^4 (around 300)	0.07	1.0×10^{-3}	2.2	40

Figure S2. Selected B_{CPL} and $|g_{\text{phos}}|$ values of optically active Pt(II) complexes. For fair comparison without artificial error, the ε_{\max} was used to calculate the B_{CPL} value. In this equation, the B_{CPL} value of all compounds should be fairly maximized without any artificial error.

General

¹H and ¹³C spectra were recorded on a JEOL ECZ-500R instrument at 500 and 125 MHz, respectively. Samples were analyzed by CDCl₃, and the chemical shift values were expressed relative to Me₄Si as an internal standard. Analytical thin layer chromatography (TLC) was performed with silica gel 60 Merck F₂₅₄ plates or silica gel 60 NH₂ F_{254S} plates. Column chromatography was performed with Wakogel C-300 SiO₂. Recyclable high-performance liquid chromatography (HPLC) was carried out on a YMC LC Forte/R. In addition, HRMS were obtained on a Bruker Daltonics microTOF II spectrometer (ESI) by using sodium formate as internal reviews. Processing and analysis of MS experimental data and generation of simulated MS spectra were carried out using Compass DataAnalysis version 4.0 SP 1 (Bruker Daltonics). The PL lifetime measurement was performed on a Hamamatsu Photonics Quantaurus-Tau fluorescence lifetime spectra meter system. UV-vis and Circular dichroism (CD) spectra were recorded on a JASCO J-1500 spectropolarimeter at room temperature. Photoluminescence (PL) and circularly polarized luminescence (CPL) spectra were recorded on a JASCO CPL-200 at room temperature. Absolute PL quantum efficiency was calculated on a JASCO FP-8500 with an ILF-835 integrating sphere.

Materials

Commercially available compounds used without purification.

NaO'Bu, pyridine, 1,4-dioxane (dehydrated), phenylboronic acid, 1,2-benzenediboronic acid bis(pinacol) ester, Pd(PPh₃)₄, K₃PO₄, Na₃PO₄, Na₂CO₃, Cs₂CO₃

Compounds prepared as described in the literature:

mono-dipyrrinatoPt(II)Cl(COE) **2**:

[31] R. Inoue, M. Yokoyama, I. Maruyama, Y. Morisaki, *Chem. Eur. J.*, **2023**, 29, e202301717.

Bisformyl(meso-aryl)dipyrromethene **3**:

[44] S. Guski, M. Albrecht, T. Willms, M. Albrecht, T. Nabeshima, F. Pan, R. Puttreddy, K. Rissanen, *Chem. Commun.*, **2017**, 53, 3213–3215.

X-ray structure determination

Crystals of *rac-anti*-**1**, (*R*_a,*R*_a)-*anti*-**1**, and **5** were analyzed using a Rigaku MicroMax-007HFM MoKa rotating anode generator equipped with VariMax optics, an AFC1 goniometer, and Saturn 724+ detector. Crystal of *syn*-**1** was analyzed using Rigaku XtaLAB-Synergy diffractometer with a HyPix-6000HE area detector and multilayer mirror-monochromated CuK α radiation ($\lambda = 1.54184 \text{ \AA}$; PhotonJet[Cu]). The reflection data for them was integrated, scaled and averaged using Rigaku CrysAlis^{PRO}. The structures were solved by a direct method (SHELXT) and refined using a full-matrix least-squares method on F2 for all reflections (SHELXL-2018/3). The calculations were performed on Olex2 program package. Crystallographic data are given in Table S2. CCDC-2386890 (for (*R*_a,*R*_a)-

anti-1), 2386891 (for *rac-anti-1*), 2386892 (for *syn-1*), and 2386893 (for **5**) contain the supplementary crystallographic data for this paper. Disordered atoms were modeled using Olex2 disorder tool. These data can be obtained free of charge from The Cambridge Crystallographic Data Centre via <https://www.ccdc.cam.ac.uk/structures/>

The authors are grateful to Professor Masako Kato and Dr Masaki Yoshida (Kwansei Gakuin University) for the scXRD analysis of *syn-1*.

For *syn-1*, multiple datasets were collected however all showed very large residuals of around 6 and -2 near the Pt atoms. Checks were made for twinning and the appropriateness of the absorption correction, however improvements were not able to be made to the refinement. The data provided confirm connectivity but no further discussion is included.

Computational methods

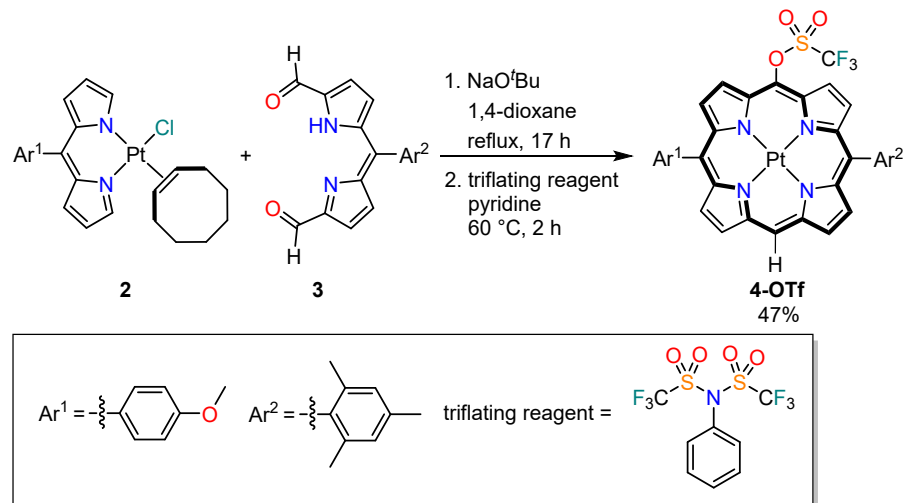
Optimized geometries of (R_a, R_a)-*anti-1* in T_1 state was obtained by using DFT calculation with the B3LYP functional, LanL2DZ^{47,48} basis set for Pt atoms, and 6-31G(d)⁴⁹ for C, H, N and O atoms included in the Gaussian 16 program package.⁵⁰ SOC-TD-DFT calculation was carried out by using Orca 6.0 program package,⁵¹ with the SARC-DKH-SVP⁵² basis set for Pt atoms and DKH-def2-SVP⁵³ basis set for C, H, and N atoms with DKH2 Hamiltonian.⁵⁴ The number of roots for singlet and triplet states were set to 181 and 180, respectively.

References

- [47] R. Bauernschmitt, R. Ahlrichs, *Chem. Phys. Lett.* **1996**, *256*, 454–464.
- [48] P. J. Hay, W. R. Wadt, *J. Chem. Phys.*, 1985, **82**, 299–310.
- [49] (a) M. M. Franci, W. J. Pietro, W. J. Hehre, J. S. Binkley, M. S. Gordon, D. J. DeFrees, J. A. Pople, *J. Chem. Phys.* **1982**, *77*, 3654–3665; (b) P. C. Hariharan, J. A. Pople, *Theor. Chim. Acta* **1973**, *28*, 213–222; (c) T. Clark, J. Chandrasekhar, G. W. Spitznagel, P. V. R. Schleyer, *J. Comput. Chem.* **1983**, *4*, 294–301.
- [50] Gaussian 16, Revision B.01, M. J. Frisch, G. W. Trucks, H. B. Schlegel, G. E. Scuseria, M. A. Robb, J. R. Cheeseman, G. Scalmani, V. Barone, G. A. Petersson, H. Nakatsuji, X. Li, M. Caricato, A. V. Marenich, J. Bloino, B. G. Janesko, R. Gomperts, B. Mennucci, H. P. Hratchian, J. V. Ortiz, A. F. Izmaylov, J. L. Sonnenberg, D. Williams-Young, F. Ding, F. Lipparini, F. Egidi, J. Goings, B. Peng, A. Petrone, T. Henderson, D. Ranasinghe, V. G. Zakrzewski, J. Gao, N. Rega, G. Zheng, W. Liang, M. Hada, M. Ehara, K. Toyota, R. Fukuda, J. Hasegawa, M. Ishida, T. Nakajima, Y. Honda, O. Kitao, H. Nakai, T. Vreven, K. Throssell, J. A. Montgomery, Jr., J. E. Peralta, F. Ogliaro, M. J. Bearpark, J. Heyd, E. N. Brothers, K. N. Kudin, V. N. Staroverov, T. A. Keith, R. Kobayashi, J. Normand, K. Raghavachari, A. P. Rendell, J. C. Burant, S. S. Iyengar, J. Tomasi, M. Cossi, J. M. Millam, M. Klene, C. Adamo, R. Cammi, J. W. Ochterski, R. L. Martin, K. Morokuma, O. Farkas, J. B. Foresman, and D. J. Fox, Gaussian, Inc., Wallingford CT, 2016.

- [51] F. Neese, *Wiley Interdiscip. Rev. Comput. Mol. Sci.* **2022**, e1606.
- [52] D. A. Pantazis, X. Y. Chen, C. R. Landis and F. Neese, *J. Chem. Theory Comput.* **2008**, *4*, 908–919.
- [53] F. Weigend, R. Ahlrichs, *Phys. Chem. Chem. Phys.* **2005**, *7*, 3297–3305.
- [54] M. Douglas, N. M. Kroll, *Ann. Phys. (NY)*, **1974**, *82*, 89–155.

Scheme S3. Synthesis of **4-OTf**.



A mixture of **2** (59.0 mg, 0.10 mmol), **3** (31.8 mg, 0.10 mmol), and NaO'Bu (9.6 mg, 0.10 mmol) were dissolved in 1,4-dioxane (100 mL) under N₂. After the mixture was reflux for 12 h, pyridine (5.0 mL) and *N*-phenylbis(trifluoromethanesulfonimide) (110.0 mg, 0.30 mmol) were added at room temperature. The mixture was stirred at 60 °C for 2 h under N₂ and then the solvent was evaporated. The residue was purified by column chromatography on SiO₂ (hexane/CH₂Cl₂ = 7:1 to 5:1 as an eluent). Further purification was carried out by gel permeation chromatography (CH₂Cl₂) to afford **4-OTf** (41.3 mg, 0.047 mmol, 47%) as a red solid. The compound **4-OTf** was air and light sensitive.

*R*_f = 0.21 (hexane/CH₂Cl₂ = 2:1 as an eluent)

¹H NMR (CDCl₃, 500 MHz) δ 1.84 (s, 6 H), 2.64 (s, 3 H), 4.12 (s, 3 H), 7.30 (s, 2 H), 7.31 (d, *J* = 8.6 Hz, 2 H), 8.07 (d, *J* = 8.6 Hz, 2 H), 8.77 (d, *J* = 4.6 Hz, 1 H), 8.81 (d, *J* = 5.2 Hz, 1 H), 8.94 (d, *J* = 4.6 Hz, 1 H), 8.99 (d, *J* = 5.2 Hz, 1 H), 9.16 (d, *J* = 4.6 Hz, 1 H), 9.18 (d, *J* = 4.6 Hz, 1 H), 9.43 (d, *J* = 5.2 Hz, 1 H), 9.45 (d, *J* = 5.2 Hz, 1 H), 10.09 (s, 1 H) ppm.

¹³C NMR (CDCl₃, 125 MHz) δ 21.5, 21.6, 55.6, 108.5, 112.5, 119.4 (q, *J*_{C-F} = 320 Hz), 121.2, 122.8, 126.2, 127.0, 127.4, 128.0, 130.6, 131.0, 131.5, 131.8, 132.16, 132.20, 132.8, 135.0, 136.3, 136.4, 136.7, 138.2, 139.0, 141.0 (three peaks), 141.3, 141.5, 141.8, 159.6 ppm;

IR(ATR): $\tilde{\nu}$ = 3052, 3011, 2951, 2925, 2849, 1736, 1604, 1510, 1458, 1423, 1247, 1221, 1334, 1017, 950, 818, 750, 698 cm⁻¹.

HRMS (ESI+): *m/z* calcd for C₃₇H₂₇F₃N₄O₄¹⁹⁵PtSNa [M+Na⁺]⁺: 898.1248; found: 898.1277.

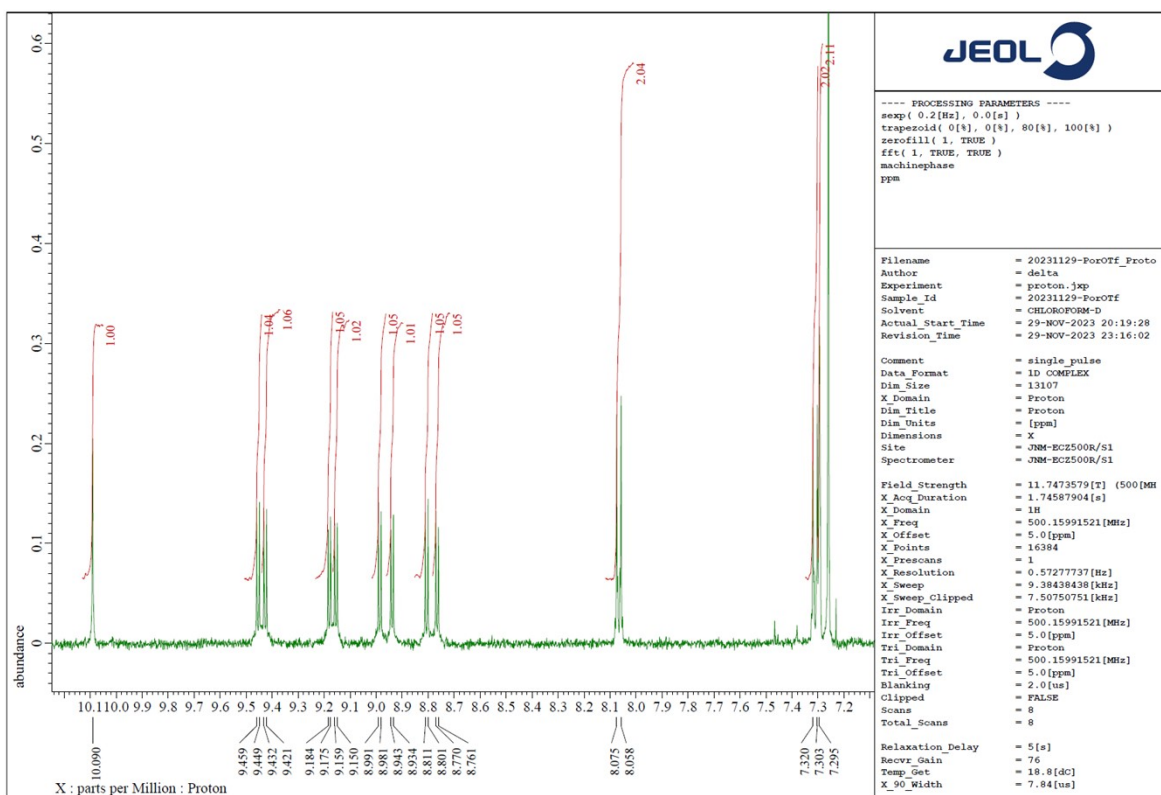
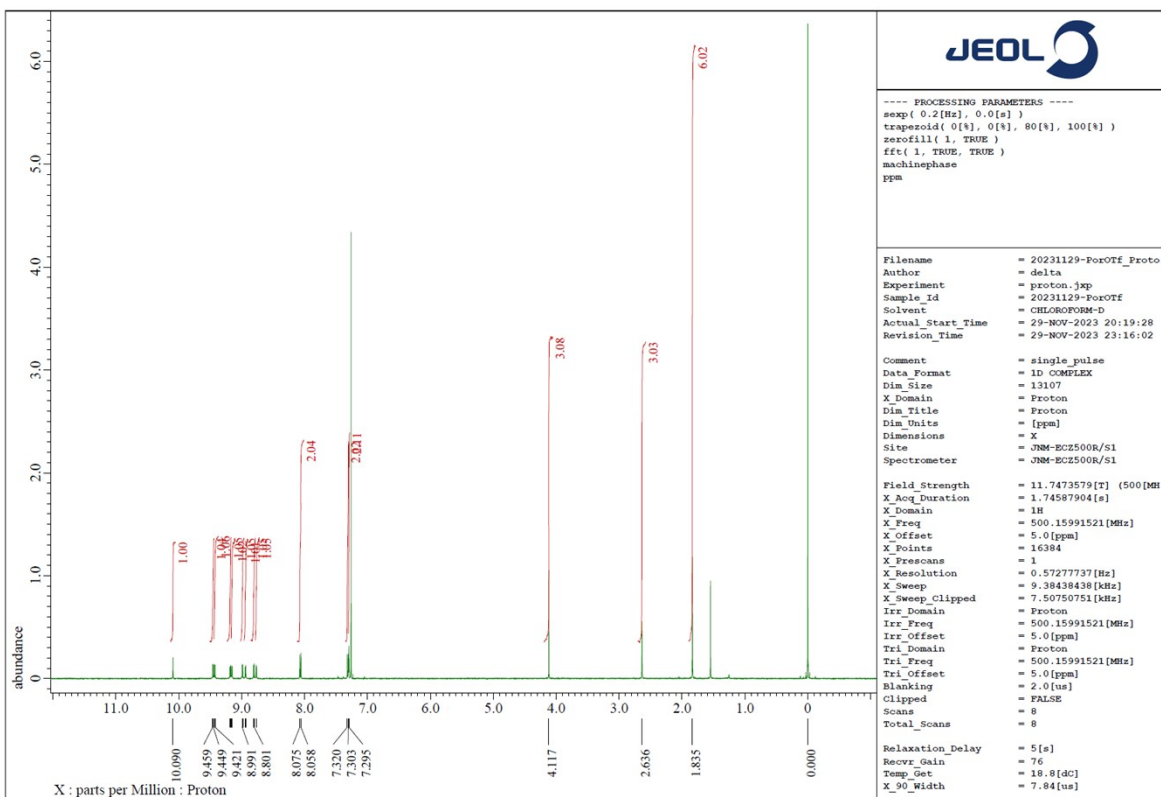


Figure S3. ^1H NMR spectra (CDCl_3 , 500 MHz) of 4-OTf.

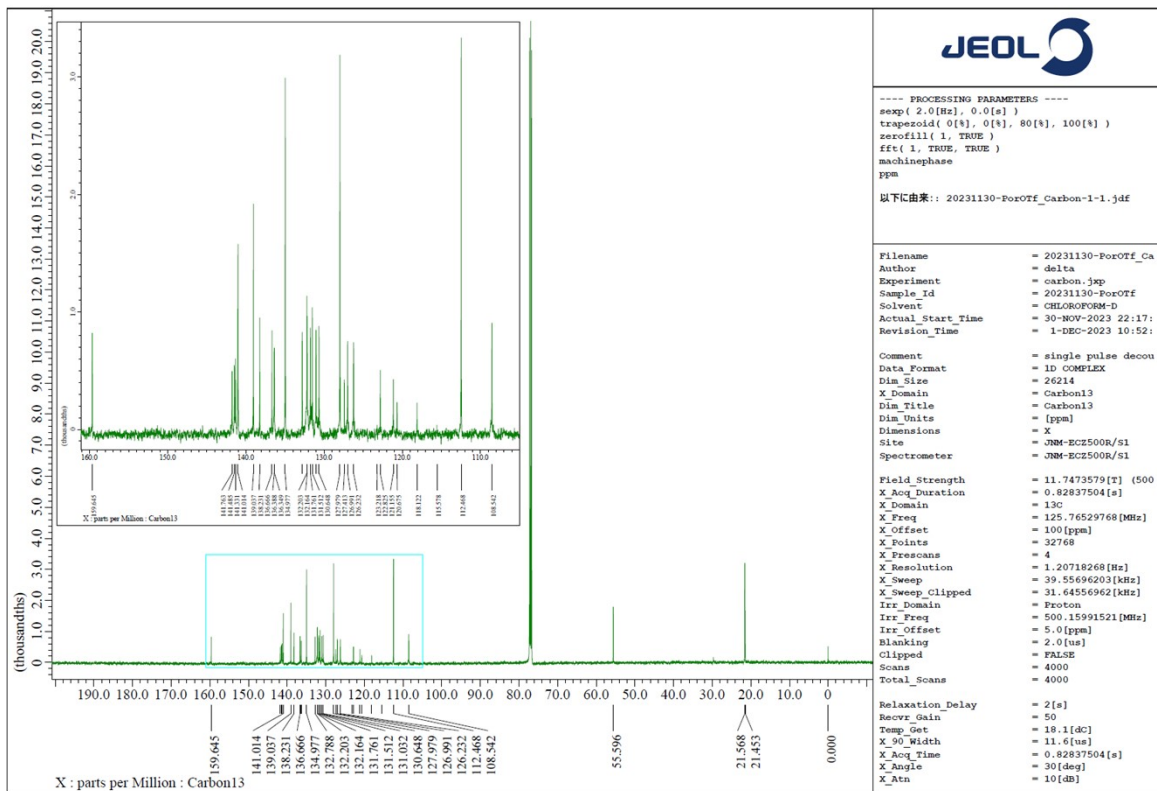


Figure S4. $^{13}\text{C}\{^1\text{H}\}$ NMR spectrum (CDCl_3 , 125 MHz) of **4-OTf**.

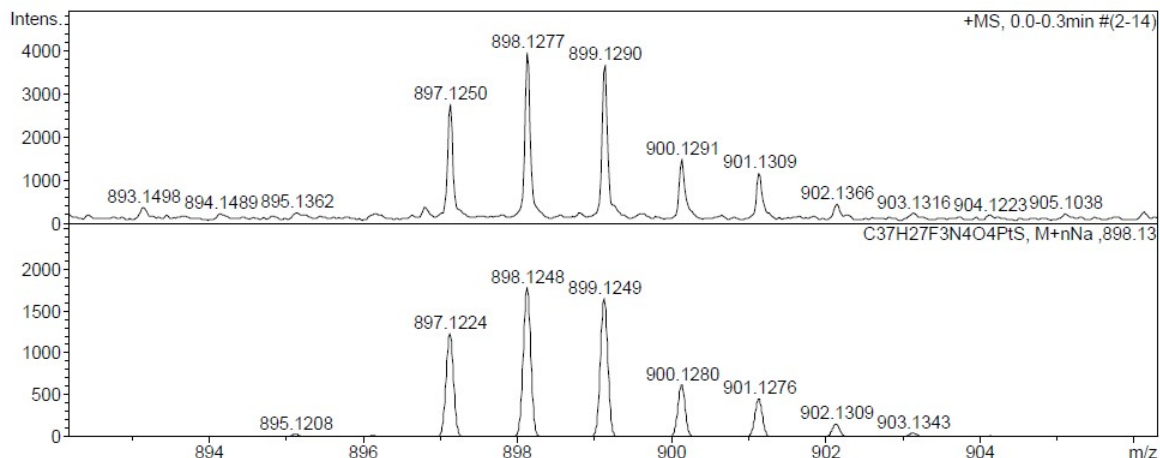
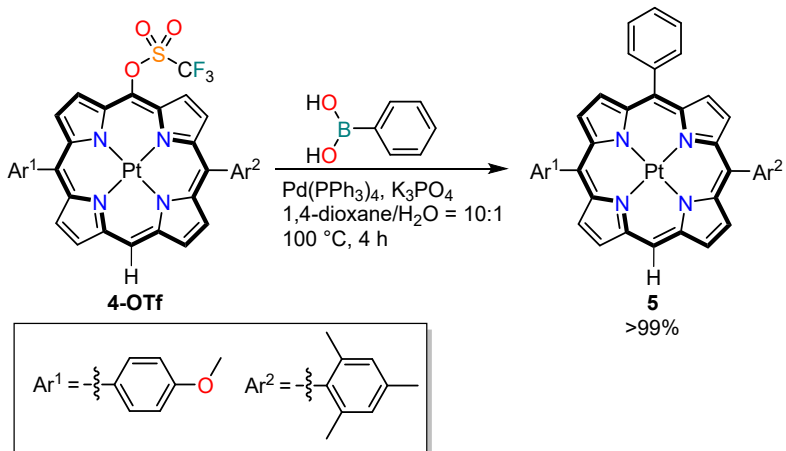


Figure S5. Mass spectra (ESI) and data of **4-OTf**. Top: experimental spectrum and bottom: theoretical spectrum.

Scheme S3. Synthesis of triaryl porphyrin **5**.



A mixture of **4-OTf** (12.3 mg, 0.014 mmol), phenyl boronic acid (3.4 mg, 0.028 mmol), $\text{Pd}(\text{PPh}_3)_4$ (1.6 mg, 0.0014 mmol, 10 mol%), and K_3PO_4 (8.9 mg, 0.42 mmol) was placed in a round bottom flask equipped with a magnetic stirring bar. After degassing the reaction mixture several times, 1,4-dioxane/ H_2O = 10/1 (1.0 mL) were added, and the reaction was carried out at 100°C for 4 h with stirring. After the reaction mixture was cooled to room temperature, H_2O and CH_2Cl_2 was added to the reaction mixture. The organic layer was separated, and then aqueous layer was extracted three times with CH_2Cl_2 and dried over MgSO_4 . MgSO_4 was removed by the filtration, and the solvent was removed by a rotary evaporator. The residue was purified by column chromatography on SiO_2 ($\text{CH}_2\text{Cl}_2/\text{hexane}$ = 7/1 to 5/1 v/v as an eluent) to afford **5** (11.3 mg, 0.0014 mmol, >99%) as an orange solid.

R_f = 0.18 (hexane/ CH_2Cl_2 = 2:1 as an eluent)

^1H NMR (CDCl_3 , 500 MHz) δ 1.84 (s, 6 H), 2.62 (s, 3 H), 4.10 (s, 3 H), 7.28 (s, 2 H), 7.29 (d, J = 8.0 Hz, 2 H), 7.69–7.76 (m, 3 H), 8.07 (d, J = 8.0 Hz, 2 H), 8.16 (d, J = 7.5 Hz, 2 H), 8.65 (d, J = 4.6 Hz, 1 H), 8.73 (d, J = 4.6 Hz, 1 H), 8.74–8.96 (m, 2 H), 8.81 (d, J = 4.6 Hz, 1 H), 8.93 (d, J = 5.2 Hz, 1 H), 9.15 (d, J = 5.2 Hz, 1 H), 9.18 (d, J = 5.2 Hz, 1 H), 10.1 (s, 1 H) ppm.

^{13}C NMR (CDCl_3 , 125 MHz) δ 21.46, 21.50, 55.6, 107.1, 112.3, 119.8, 121.6, 122.3, 126.7, 127.78, 127.83, 129.43, 130.1, 130.5, 130.6, 130.7, 131.2 (two peaks were overlapped), 131.3, 133.6, 133.85, 134.92, 137.4, 137.8, 139.2, 140.35, 140.41 (two peaks were overlapped), 140.60, 140.63, 140.9, 141.1, 141.5 (two peaks were overlapped), 159.4 ppm.

IR(ATR): $\tilde{\nu}$ = 3101, 3049, 2984, 2954, 2925, 2868, 2830, 1612, 1510, 1450, 1247, 1096, 1017, 795, 746, 702 cm^{-1} .

HRMS (ESI $+$): m/z calcd for $\text{C}_{42}\text{H}_{32}\text{N}_4\text{O}^{195}\text{PtNa}$ [$\text{M}+\text{Na}^+$] $^+$: 826.2119; found: 826.2121.

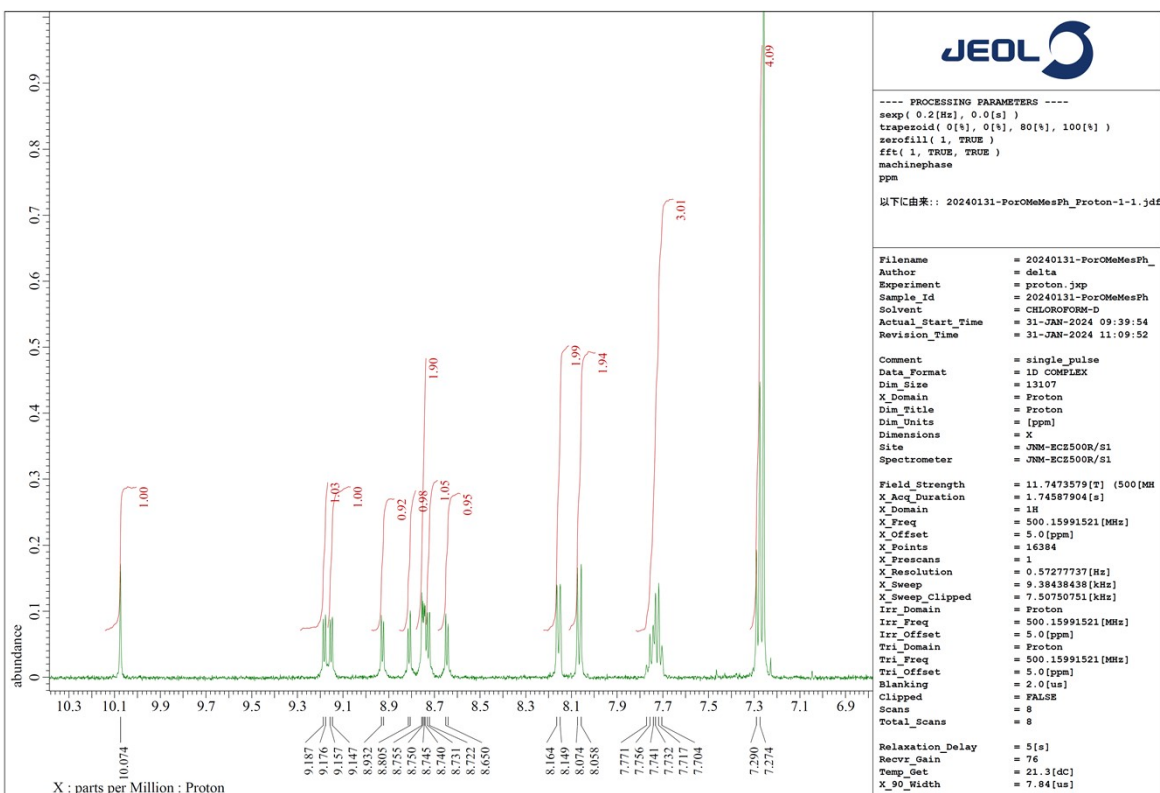
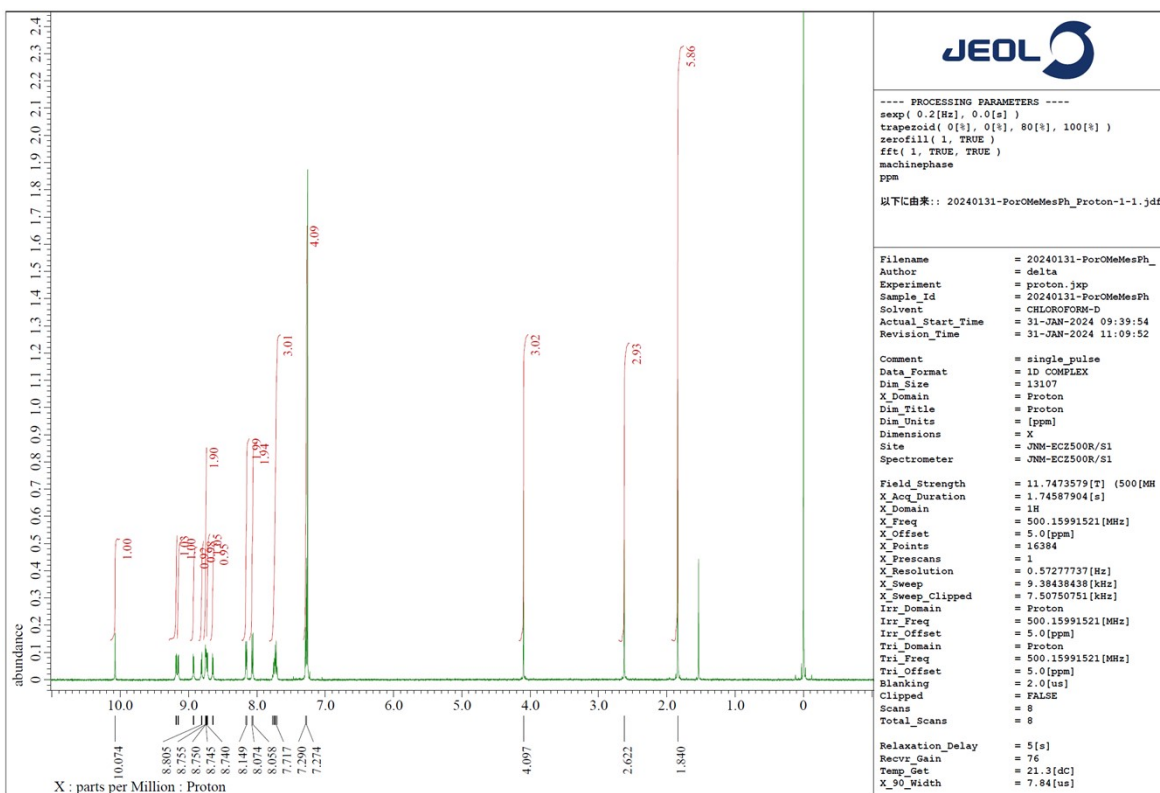


Figure S6. ^1H NMR spectra (CDCl_3 , 500 MHz) of **5**.

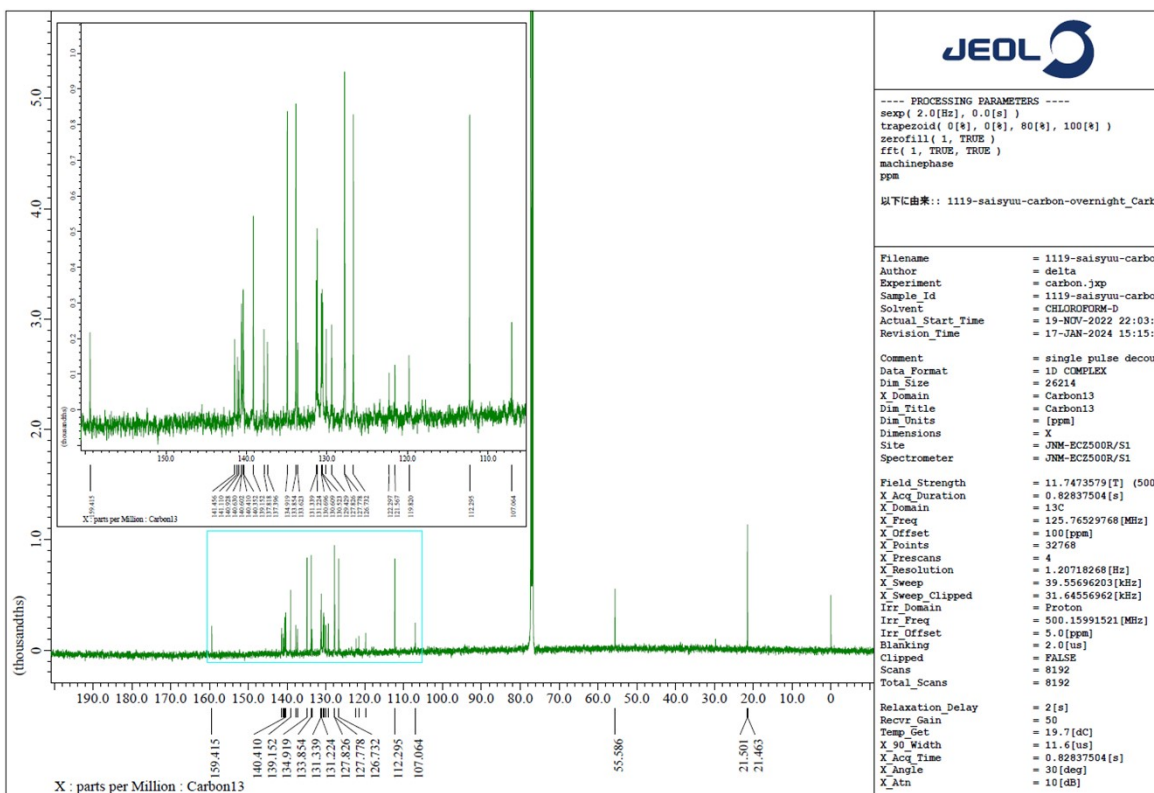


Figure S7. $^{13}\text{C}\{\text{H}\}$ NMR spectrum (CDCl_3 , 125 MHz) of **5**.

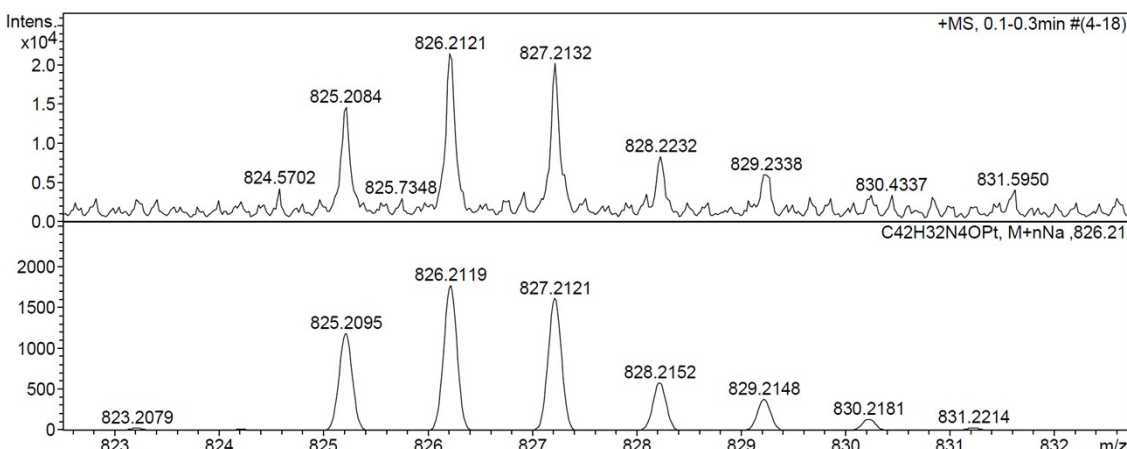


Figure S8. Mass spectra (ESI) and data of **5**. Top: experimental spectrum and bottom: theoretical spectrum.

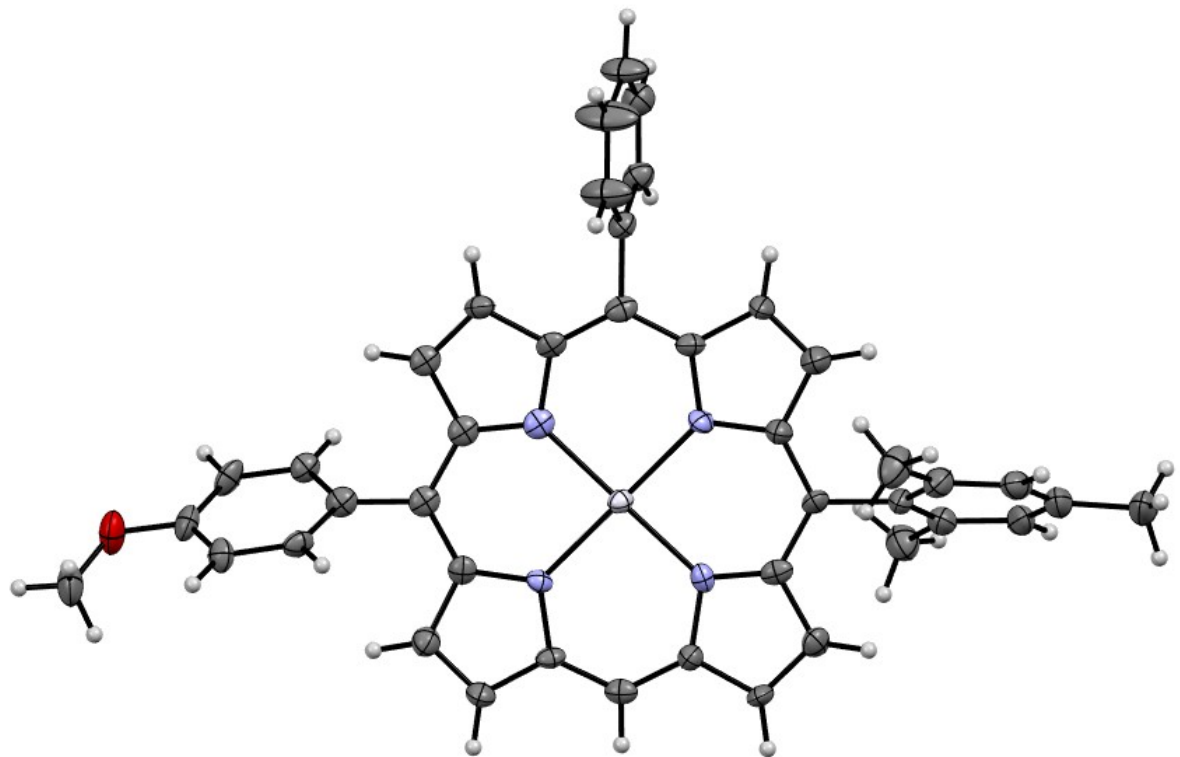
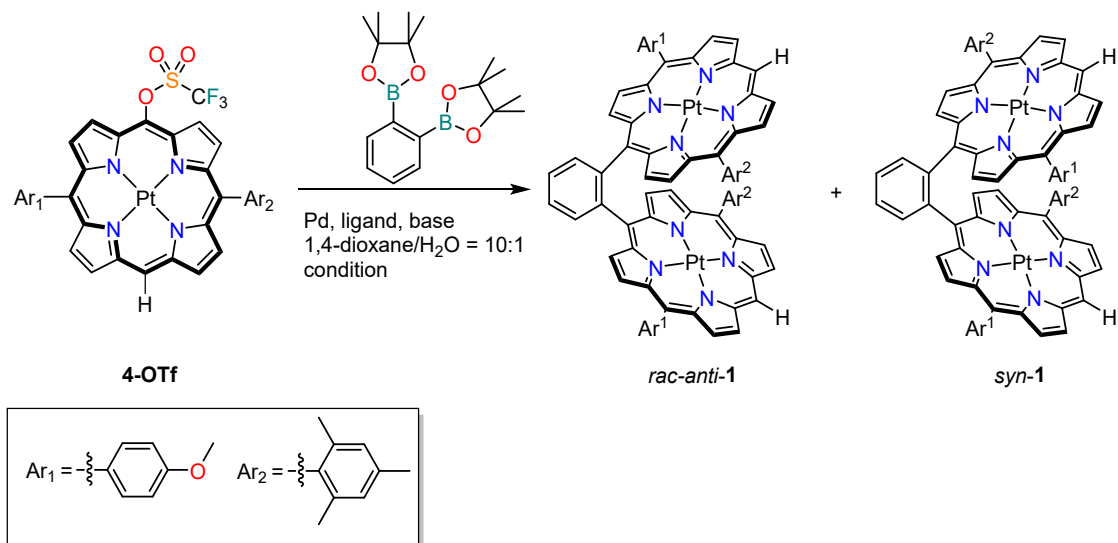


Figure S9. ORTEP drawing of **5** (CCDC-2386893). Thermal ellipsoids are drawn at the 50% probability level. C: gray, H: off-white, N: blue, O: red, and Pt: white.

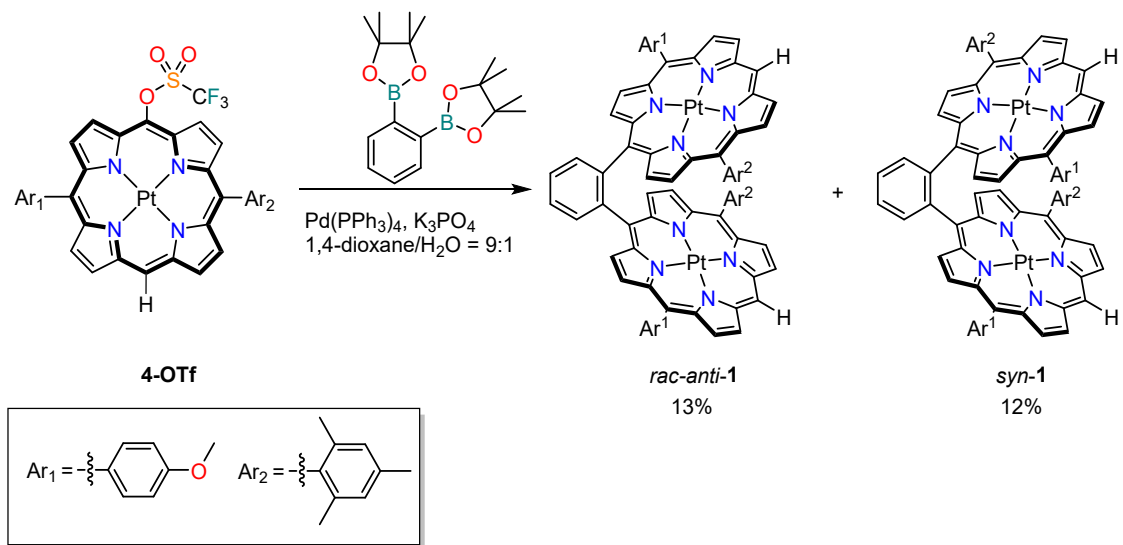
Table S1. Optimization of reaction condition for synthesis of **1**.



Entry	Pd, ligand	Base	Conc.	Condition	NMR Yield ^[a] [%]	
					<i>anti-1</i>	<i>syn-1</i>
1	Pd(PPh ₃) ₄ 20 mol%	K ₃ PO ₄ 3 eq.	0.01 M	100 °C, 17 h	10	17
2	Pd(PPh ₃) ₄ 20 mol%	Na ₃ PO ₄ 3 eq.	0.01 M	100 °C, 17 h	7	9
3	Pd(PPh ₃) ₄ 20 mol%	Na ₂ CO ₃ 5 eq.	0.01 M	100 °C, 17 h	7	9
4	Pd(PPh ₃) ₄ 20 mol%	Cs ₂ CO ₃ 5 eq.	0.01 M	100 °C, 17 h	6	8
5 ^b	Pd(PPh ₃) ₄ 20 mol%	CsF 10 eq.	0.08 M	100 °C, 7 h	0	0
6	Pd(PPh ₃) ₄ 4 mol%	K ₃ PO ₄ 3 eq.	0.01 M	100 °C, 10 h	2	5
7	Pd(PPh ₃) ₄ 20 mol%	K ₃ PO ₄ 3 eq.	0.08 M	100 °C, 7 h	12	10
8	Pd ₂ (dba) ₃ 10 mol%, SPhos 20 mol%	K ₃ PO ₄ 3 eq.	0.06 M	100 °C, 7 h	0	0
9	Pd ₂ (dba) ₃ 10 mol%, dppf 10 mol%	K ₃ PO ₄ 3 eq.	0.04 M	100 °C, 7 h	4	2
10	Pd ₂ (dba) ₃ 10 mol%, dppm 10 mol%	K ₃ PO ₄ 3 eq.	0.04 M	100 °C, 7 h	3	3

[a] Yield were determined by ¹H NMR spectra of the crude products after CH₂Cl₂/water extraction.
[2.2]Paracyclophane was used as an internal standard. [b] Solvent: 1,4-dioxane (anhydrous)

Scheme S4. Synthesis of porphyrin dimer **1**.



A mixture of **4-OTf** (35.1 mg, 0.040 mmol), 1,2-benzenediboronic acid bis(pinacol) ester (6.6 mg, 0.020 mmol), $\text{Pd}(\text{PPh}_3)_4$ (9.3 mg, 0.080 mmol), and K_3PO_4 (25.5 mg, 0.12 mmol) was placed in a round bottom flask equipped with a magnetic stirring bar. After degassing the reaction mixture several times, $1,4\text{-dioxane}/\text{H}_2\text{O} = 10/1$ (0.5 mL) were added, and the reaction was carried out at 100°C for 7 h with stirring. After the reaction mixture was cooled to room temperature, H_2O was added to the reaction mixture. The organic layer was separated, and then aqueous layer was extracted three times with CH_2Cl_2 and dried over MgSO_4 . MgSO_4 was removed by the filtration, and the solvent was removed by a rotary evaporator. The residue was purified by column chromatography on SiO_2 ($\text{CH}_2\text{Cl}_2/\text{hexane} = 10/2$ to $1/1$ v/v as an eluent) and by gel permeation chromatography (CH_2Cl_2 as an eluent) to afford a mixture of *rac-anti-1* and *syn-1* as a red solid. Further purification was carried out by chiral HPLC ($\text{CH}_2\text{Cl}_2/\text{hexane} = 2/8$) to afford *rac-anti-1* (4.0 mg, 0.0026 mmol, 13%) and *syn-1* (3.6 mg, 0.0024 mmol, 12%) as a red crystal. Optical resolution of *rac-anti-1* was carried out using chiral HPLC (${}^i\text{PrOH}/\text{hexane} = 7/3$ as an eluent).

$R_f = 0.71$ (CH_2Cl_2 as an eluent).

***anti*-1**

¹H NMR (CDCl₃, 500 MHz) δ -0.20 (s, 6 H), 1.49 (s, 6 H), 2.60 (s, 6 H), 4.10 (s, 6 H), 6.96 (s, 2 H), 7.03 (dd, *J* = 8.0, 2.9 Hz, 2 H), 7.06–7.12 (m, 6 H), 7.03 (dd, *J* = 8.0, 2.3 Hz, 2 H), 7.86 (d, *J* = 5.2 Hz, 2 H), 8.15 (d, *J* = 4.6 Hz, 2 H), 8.17 (d, *J* = 5.2 Hz, 2 H), 8.27 (dd, *J* = 5.4, 4.0 Hz, 2 H), 8.46 (d, *J* = 5.2 Hz, 2 H), 8.67 (d, *J* = 5.2 Hz, 2 H), 8.76 (d, *J* = 4.6 Hz, 2 H), 8.80 (dd, *J* = 5.4, 4.0 Hz, 2 H), 8.76 (d, *J* = 5.2 Hz, 2 H), 9.06 (d, *J* = 5.2 Hz, 2 H), 9.53 (s, 2 H) ppm.

¹³C NMR (CDCl₃, 125 MHz) δ 19.6, 21.1, 21.4, 55.6, 106.6, 111.7, 112.0, 118.6, 119.9, 120.5, 127.3 (three pwaks), 127.4, 127.6, 129.0, 129.2, 130.0, 130.2, 130.5, 130.6, 131.4, 133.3, 133.4, 134.3, 134.7, 137.0, 137.3, 138.3, 139.1, 139.3, 139.4, 139.5, 139.6, 139.8, 140.0, 140.3, 144.7, 159.1 ppm.

IR(ATR): $\tilde{\nu}$ = 3101, 3056, 2992, 2954, 2925, 2853, 1736, 1608, 1510, 1454, 1288, 1243, 1179, 1100, 1070, 1017, 694 cm⁻¹.

HRMS (ESI+): *m/z* calcd for C₇₈H₅₈N₈O₂¹⁹⁵PtNa [M+Na⁺]⁺: 1551.3867; found: 1551.3844.

*R*_f = 0.71 (CH₂Cl₂ as an eluent).

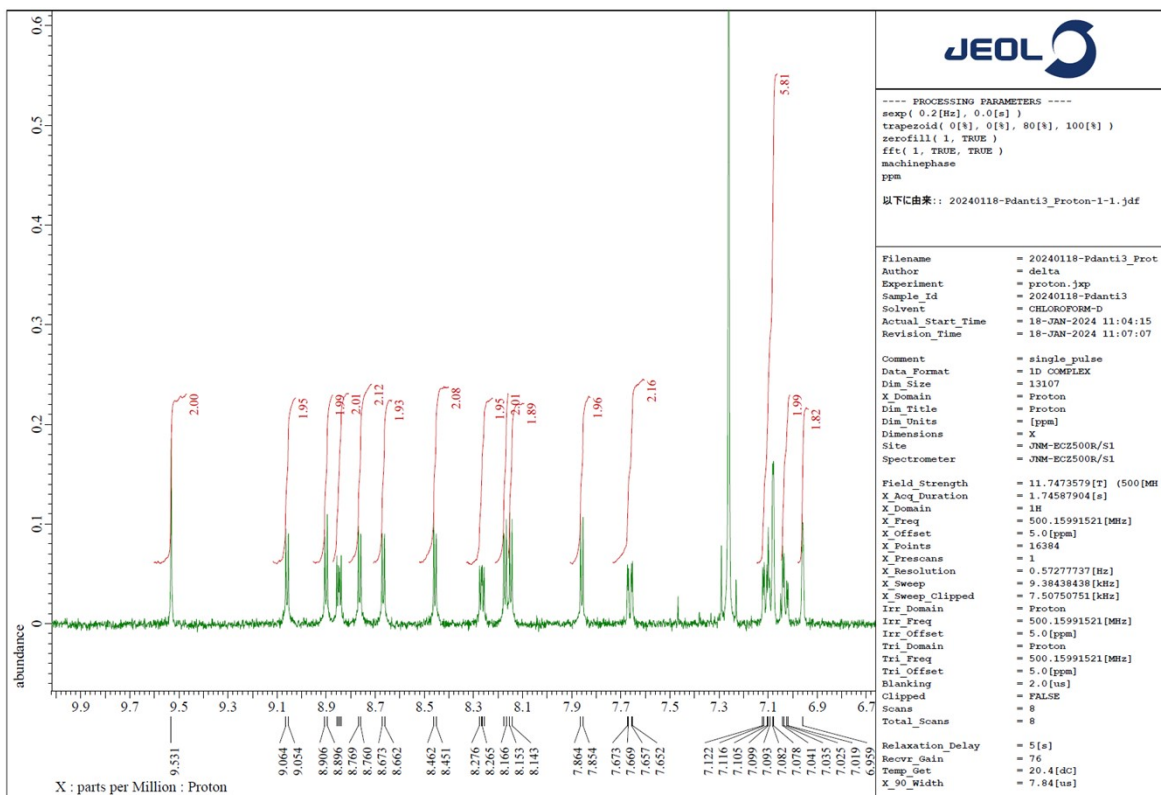
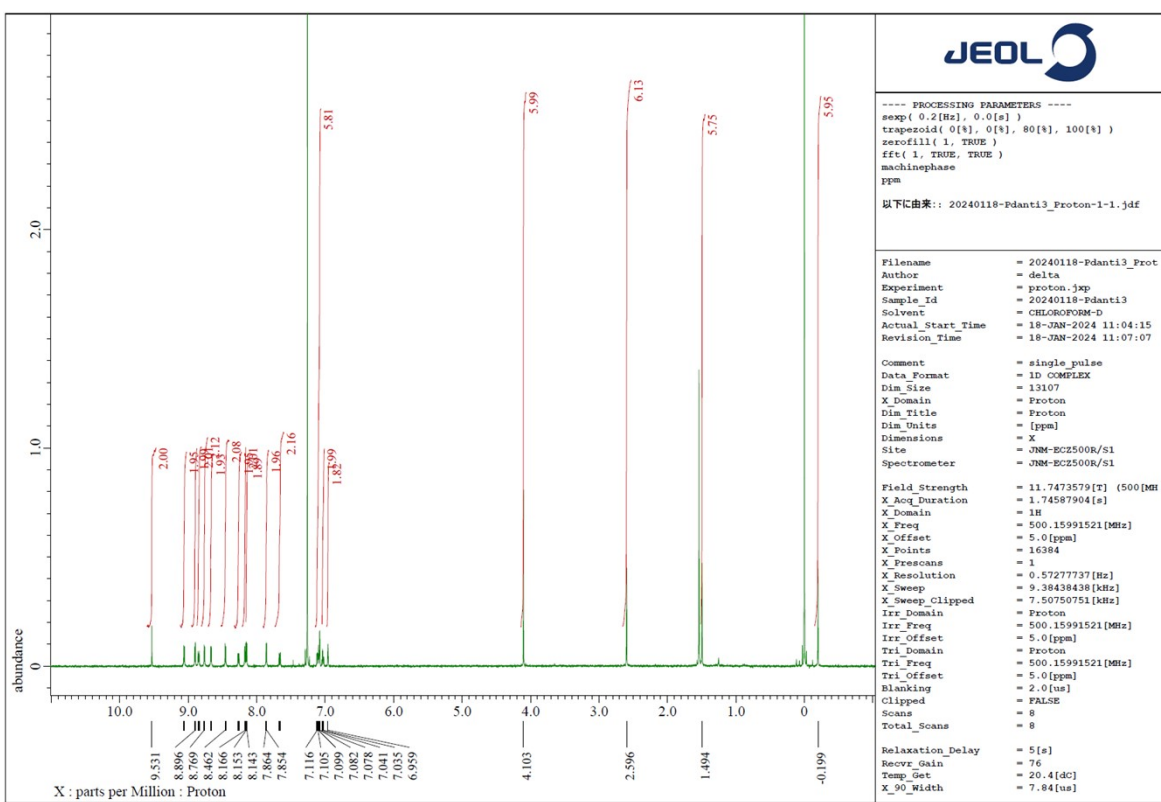


Figure S10. ^1H NMR spectra (CDCl_3 , 500 MHz) of *anti*-1.

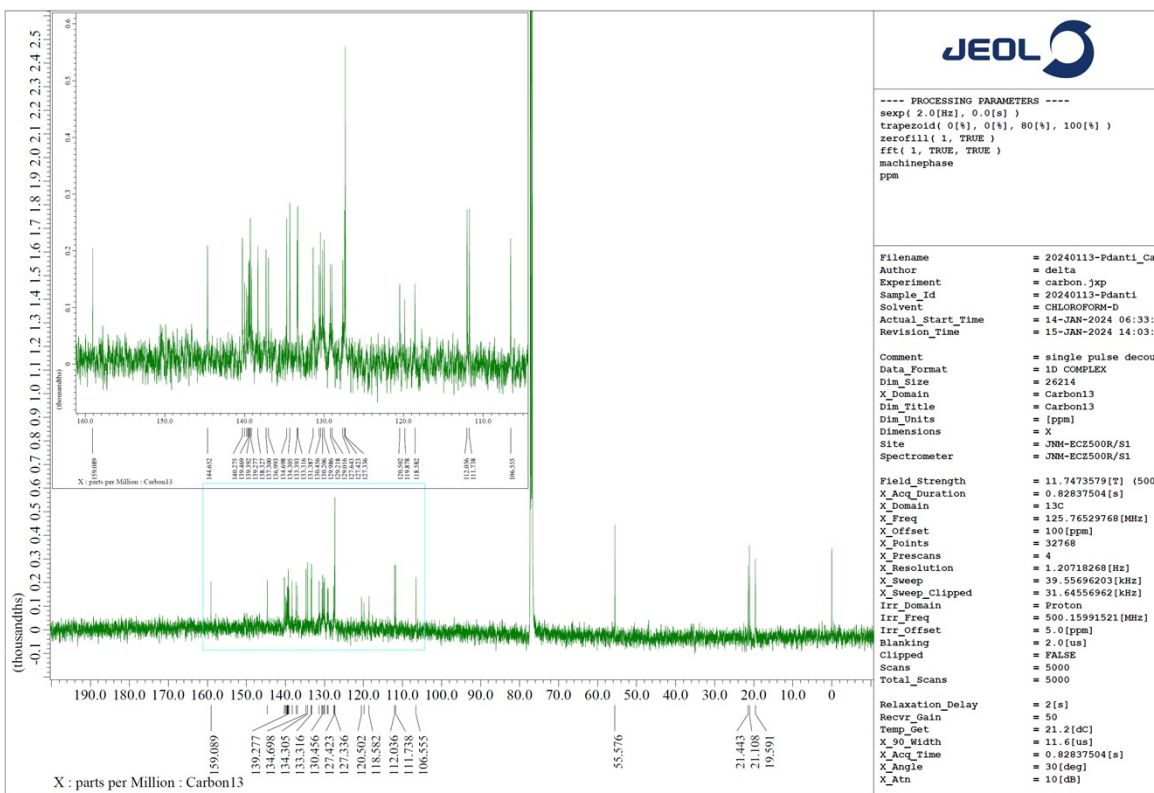


Figure S11. $^{13}\text{C}\{^1\text{H}\}$ NMR spectrum (CDCl_3 , 125 MHz) of *anti-1*.

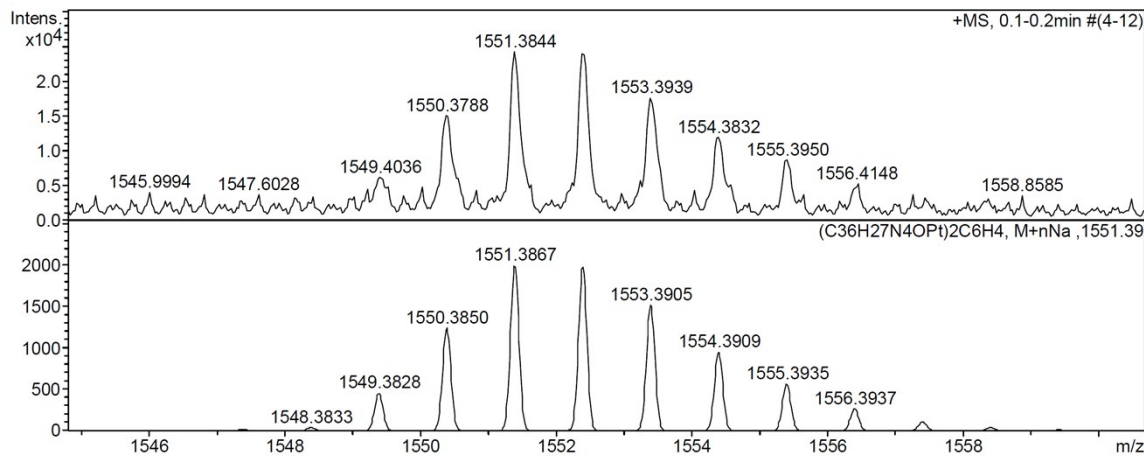


Figure S12. Mass spectra (ESI) and data of *anti-1*. Top: experimental spectrum and bottom: theoretical spectrum.

syn-1

¹H NMR (CDCl₃, 500 MHz) δ 0.29 (s, 6 H), 1.43 (s, 6 H), 2.55 (s, 6 H), 4.06 (s, 6 H), 6.82 (dd, *J* = 8.0, 2.3 Hz, 2 H), 6.88 (s, 2 H), 6.83 (dd, *J* = 8.0, 2.9 Hz, 2 H), 7.05 (s, 2 H), 7.09 (dd, *J* = 8.6, 2.9 Hz, 2 H), 7.65 (dd, *J* = 8.6, 2.3 Hz, 2 H), 7.65 (dd, *J* = 8.6, 2.3 Hz, 2 H), 7.87 (d, *J* = 5.2 Hz, 2 H), 8.11 (d, *J* = 4.6 Hz, 2 H), 8.22 (d, *J* = 4.6 Hz, 2 H), 8.26 (dd, *J* = 5.7, 4.0 Hz, 2 H), 8.44 (d, *J* = 4.6 Hz, 2 H), 8.73 (d, *J* = 5.2 Hz, 2 H), 8.75 (d, *J* = 5.2 Hz, 2 H), 8.84 (dd, *J* = 5.7, 4.0 Hz, 2 H), 8.97 (d, *J* = 5.2 Hz, 2 H), 9.02 (d, *J* = 5.2 Hz, 2 H), 9.56 (s, 2 H) ppm.

¹³C NMR (CDCl₃, 125 MHz) δ 20.4, 21.1, 21.4, 55.5, 106.6, 111.7, 112.0, 118.7, 120.2, 120.5, 127.2, 127.3, 127.5, 128.1, 129.09, 129.13, 129.9, 130.2, 130.6, 130.7, 131.2, 133.2, 134.3, 1134.4, 134.7, 136.9, 137.2, 138.5, 138.8, 139.2, 139.5 (two peaks), 139.6, 139.9, 140.1, 140.2, 140.3, 144.3, 159.0 ppm;

IR(ATR): $\tilde{\nu}$ = 3067, 2996, 2958, 2925, 2868, 2853, 2826, 1743, 1728, 1608, 1510, 1454, 1243, 1108, 1021, 792, 694 cm⁻¹.

HRMS (ESI+): *m/z* calcd for C₇₈H₅₈N₈O₂¹⁹⁵PtNa [M+Na⁺]⁺: 1551.3867; found: 1551.3830.

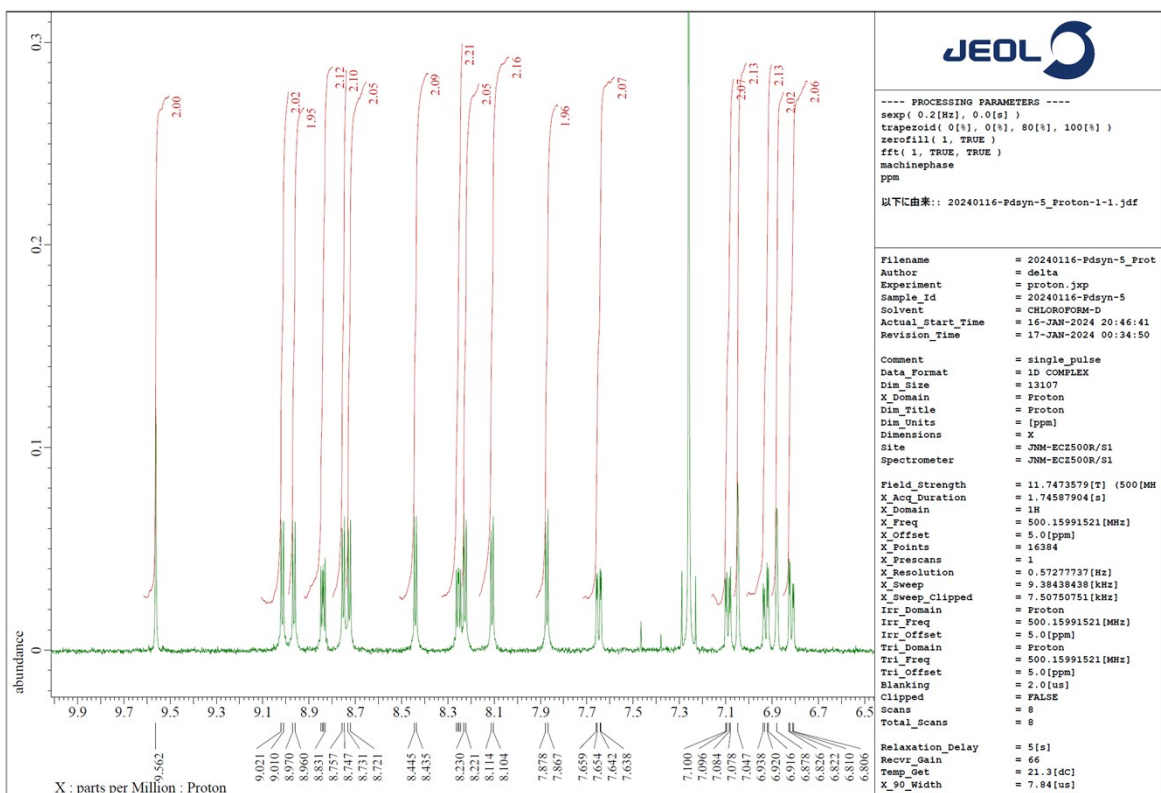
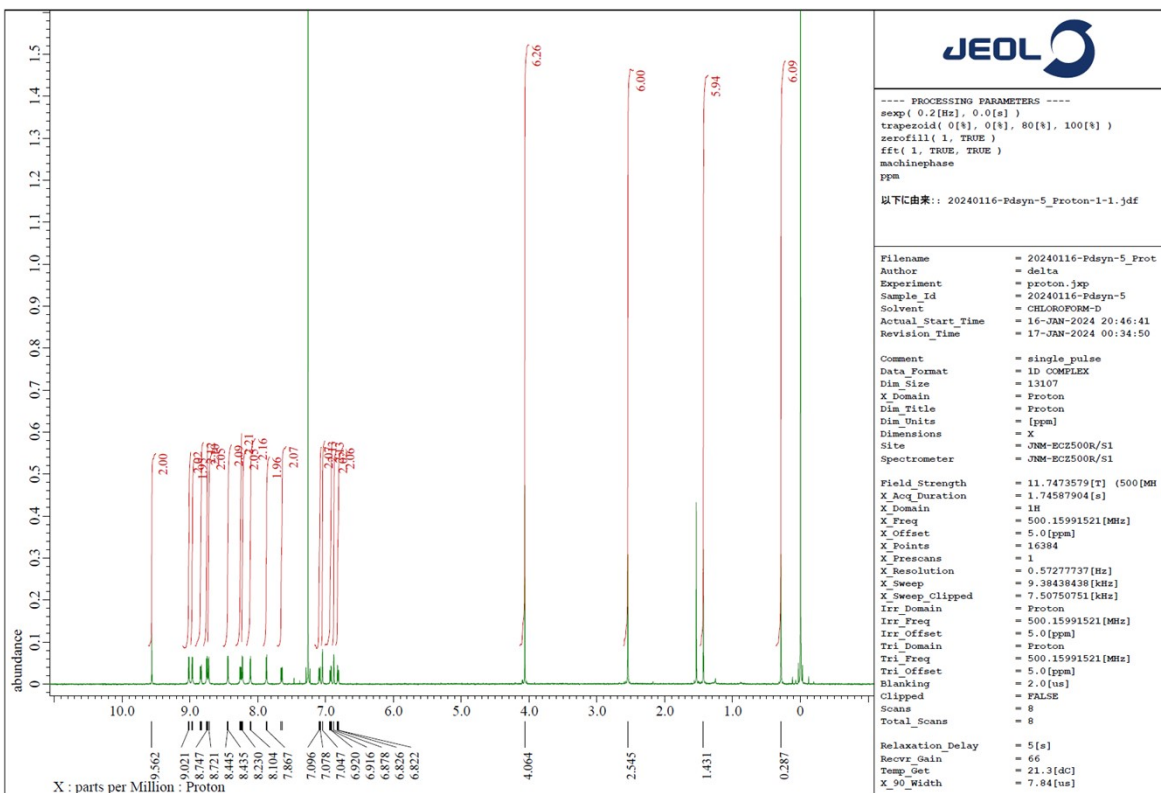


Figure S13. ^1H NMR spectra (CDCl₃, 500 MHz) of *syn-1*.

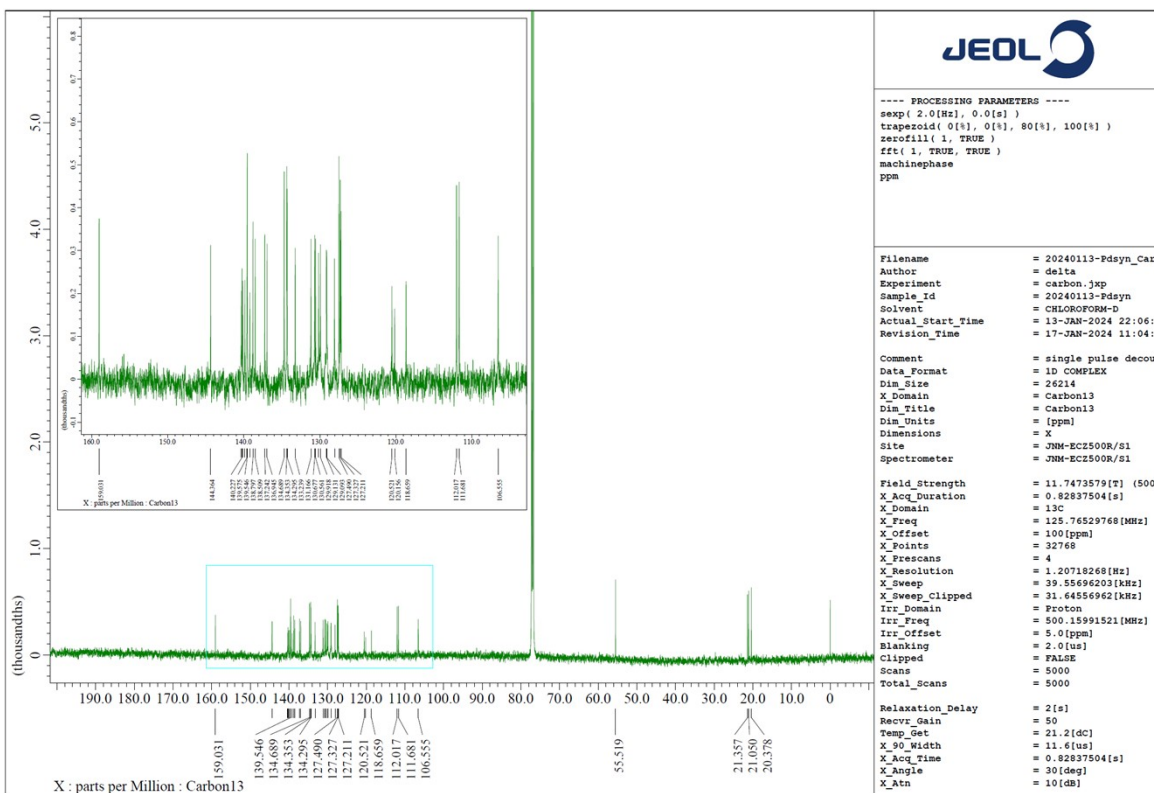


Figure S14. $^{13}\text{C}\{^1\text{H}\}$ NMR spectrum (CDCl_3 , 125 MHz) of *syn-1*.

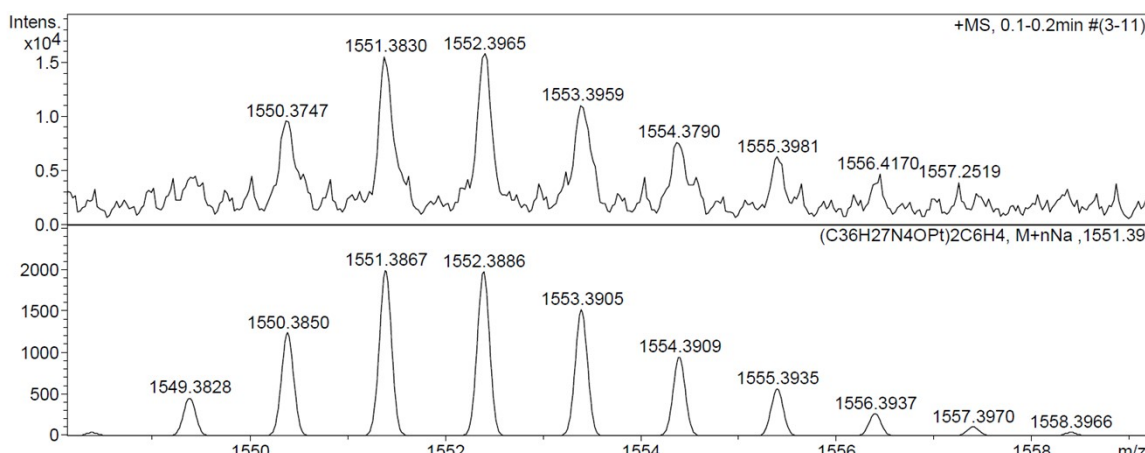


Figure S15. Mass spectra (ESI) and data of *syn-1*. Top: experimental spectrum and bottom: theoretical spectrum.

Table S2. Crystallographic data and structure refinements for **5**, *rac-anti-1*, (*R_aR_a*)-*anti-1*, and *syn-1*.

Molecule	5	<i>rac-anti-1</i>	(<i>R_aR_a</i>)- <i>anti-1</i> •4CHCl ₃	<i>syn-1</i> •0.5hexane•CHCl ₃
Formula	C ₄₂ H ₃₂ N ₄ OPt	C ₇₈ H ₅₈ N ₈ O ₂ Pt ₂	C ₈₂ H ₆₂ Cl ₁₂ N ₈ O ₂ Pt ₂	C ₈₂ H ₆₆ Cl ₃ N ₈ O ₂ Pt ₂
Formula weight	803.80	1529.50	2006.97	1691.95
Temperature (K)	150	150	150	150
Crystal color, habit	red, plate	orange, needle	orange, plate	red, plate
Crystal size, mm	0.05× 0.05 × 0.01	0.30× 0.05 × 0.01	0.50× 0.30 × 0.20	0.05× 0.02 × 0.02
Crystal system	triclinic	triclinic	orthorhombic	triclinic
Space group	<i>P</i> -1 (#2)	<i>P</i> -1 (#2)	<i>P</i> 2 ₁ 2 ₁ (#18)	<i>P</i> -1 (#2)
<i>a</i> , Å	10.1467(5)	11.5446(3)	19.3188(3)	11.3270(2)
<i>b</i> , Å	17.0883(8)	17.1268(5)	19.1158(3)	16.6957(2)
<i>c</i> , Å	21.2534(7)	17.3718(5)	10.62740(10)	17.5885(3)
α , deg	111.170(4)	71.885(2)	90	94.9910(10)
β , deg	93.759(3)	72.120(2)	90	93.2430(10)
γ , deg	106.032(4)	77.570(2)	90	90.9970(10)
<i>V</i> , Å ³	3246.1(3)	3079.51(16)	3924.64(9)	3307.45(9)
<i>Z</i> value	4	2	2	2
<i>D</i> _{calcd} , g cm ⁻³	1.645	1.649	1.698	1.699
μ (MoK α), cm ⁻¹	43.64	45.95	40.23	18.736 (CuK α)
<i>F</i> (000)	1592.0	1508.0	1972.0	1674.0
2 θ _{max} , deg	52.044	50.696	59.134	152.796
No. of reflections measured	23877	21430	38932	46056
No. of observed reflections	12530	11090	10138	13284
No. of variables	873	863	526	914
<i>R</i> ₁ (I > 2 σ (I)) ^[a]	0.0517	0.0576	0.0307	0.0627
w <i>R</i> ₂ (all reflns) ^[b]	0.1212	0.1429	0.0784	0.1788
Goodness of fit	1.063	1.019	1.030	1.098
Flack parameter	-	-	-0.025(4)	-
Recrystallization solvent	CH ₂ Cl ₂ /MeOH	CH ₂ Cl ₂ /CH ₃ CN	CHCl ₃ /hexane	CHCl ₃ /hexane

[a] $R_1 = \Sigma(|F_o| - |F_c|) / \Sigma(|F_o|)$. [b] $wR_2 = [\sum[w(F_o^2 - F_c^2)^2] / \sum w(F_o^2)^2]^{1/2}$.

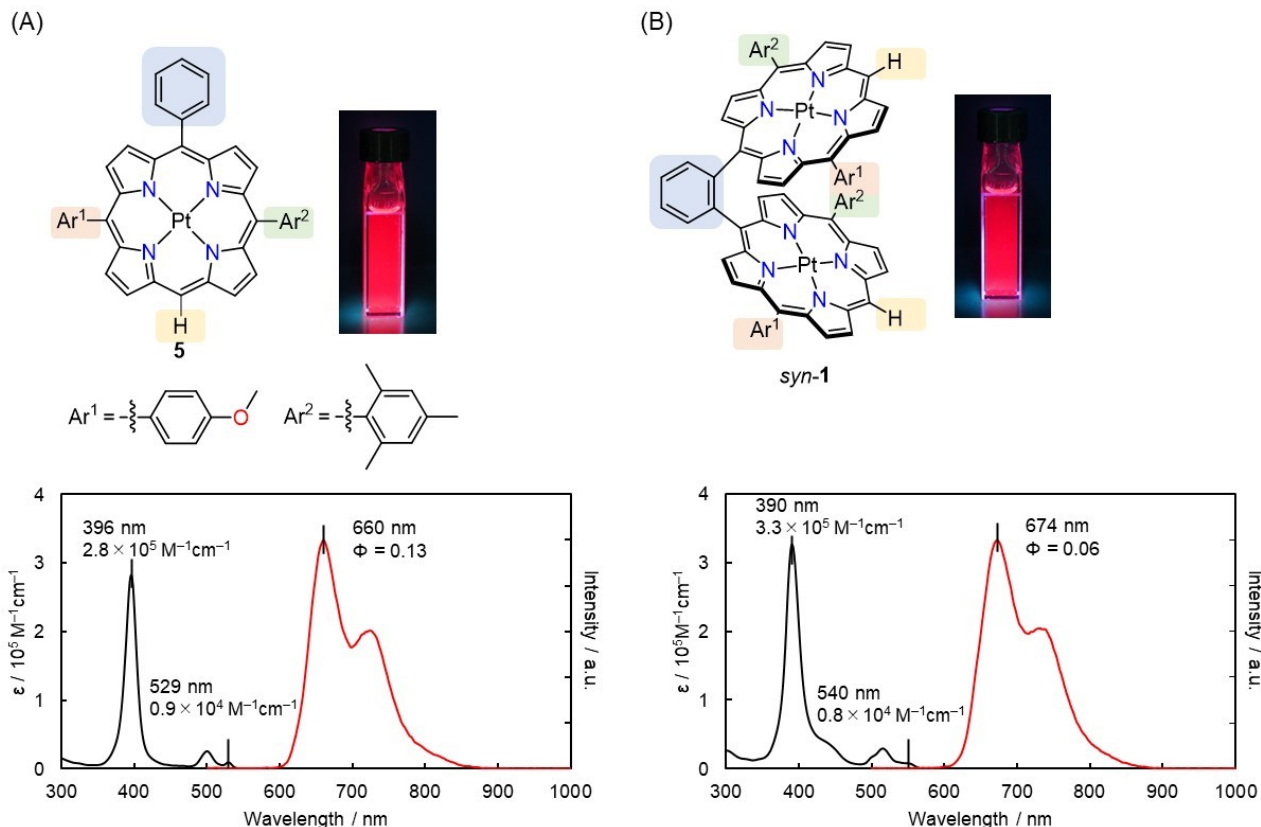


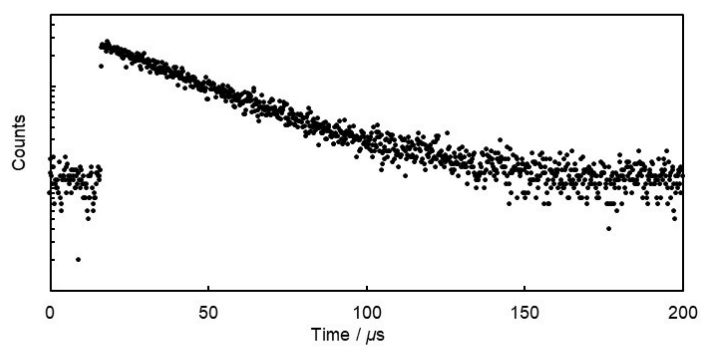
Figure S16. UV-vis (black line) and PL spectra (red line) of (A) **5** ($1.0 \times 10^{-5} \text{ M}$) and (B) *syn*-**1** ($5.0 \times 10^{-6} \text{ M}$) in toluene.

Table S2. Photophysical data for *anti*-**1**, *syn*-**1** and **5**.^[a]

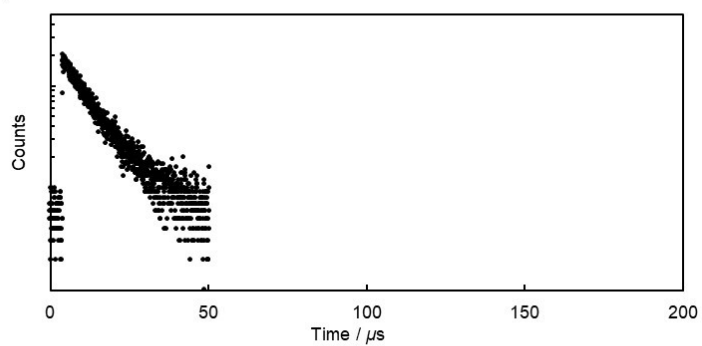
Compound	Soret band [nm] ($\epsilon \times 10^5 / \text{M}^{-1}\text{cm}^{-1}$)	Q band [nm] ($\epsilon \times 10^4 / \text{M}^{-1}\text{cm}^{-1}$)	$\lambda_{\text{lum},\text{max}}$ [nm]	$\Phi^{[b]}$	$\tau [\mu\text{s}] (\chi^2)$	k_r [10^3 s^{-1}]	k_{nr} [10^4 s^{-1}]
<i>anti</i> - 1	387 (4.13)	509 (0.35), 542 (0.11)	679	0.07	31.0 (1.0)	2.3	3.0
<i>syn</i> - 1	390 (3.26)	515 (0.30), 540 (sh, 0.08)	674	0.06	8.8 (1.0)	6.8	10.7
5	396 (2.81)	500 (0.25), 529 (0.09)	660	0.13	42.5 (1.0)	3.1	2.0

[a] Emission spectra, quantum efficiencies, and emission decays were measured in degassed toluene solution ($6.0 \times 10^{-6} \text{ M}$ for **1** and $1.0 \times 10^{-5} \text{ M}$ for **5**) at room temperature. [b] Determined by the absolute method using an integrating sphere.

(A)



(B)



(C)

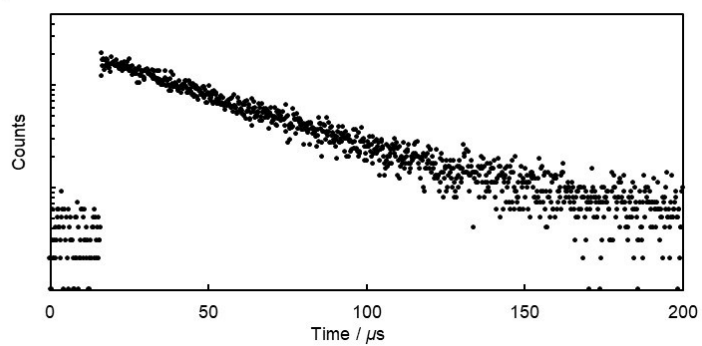


Figure S17. Emission decay curves for (A) *anti*-**1**, (B) *syn*-**1**, and (C) **5** in degassed toluene (5.0×10^{-6} M for **1**, and 1.0×10^{-5} M for **5**) monitored at each λ_{max} ($\lambda_{\text{ex}} = 405$ nm).

Equations S(1)–S(3) for phosphorescent dissymmetry factor g_{phos} .

$$g_{\text{phos},T} = C_1 g_{1,T} + C_2 g_{2,T} + C_3 g_{3,T} \# S(1)$$

$$C_i = \frac{k_i \rho_{i,T}}{(k_1 \rho_{1,T} + k_2 \rho_{2,T} + k_3 \rho_{3,T})} \# S(2)$$

$$\rho_{i,T} = \frac{\exp\left(-\frac{\Delta E_{i1}}{kT}\right)}{\left[\exp\left(-\frac{\Delta E_{31}}{kT}\right) + \exp\left(-\frac{\Delta E_{21}}{kT}\right) + 1\right]} \# S(3)$$

In these equations, $g_{i,T}$ ($i = 1, 2, 3$) is the dissymmetry factor of each triplet sublevel at temperature T; C_i ($i = 1, 2, 3$), k_i ($i = 1, 2, 3$), and $\rho_{i,T}$ are the coefficient, radiative rate constant, and Boltzmann population of each triplet sublevel, respectively; ΔE_{12} represents the energy difference between $T_{1,1}$ and $T_{1,2}$; ΔE_{13} represents the difference between $T_{1,1}$ and $T_{1,3}$; k is the Boltzmann constant.

Equations S(4) for dissymmetry factor g_{lum} .

$$g_{\text{lum}} = 4|\mu||m|\cos\theta/(|\mu|^2 + |m|^2) \# S(4)$$

To increase g_{lum} value, the transition containing small μ , large m value, and $\theta = 0$ or 180° are required.

- a) *Circular Dichroism 2nd ed.* (Eds.: N. Berova, K. Nakanishi, R. W. Woody, Wiley-VCH: Toronto, 2000; b) J. P. Riehl, F. S. Richardson, *Chem. Rev.* **1986**, 86, 1-16; c) J. P. Riehl, F. Muller, *Comprehensive Chiroptical Spectroscopy*, Wiley and Sons: New York, 2012.

Table S3. Major configurations and components of SOC transition for (R_a, R_a) -anti-1 (The threshold of weight is 0.000050).

State	Weight	Component
SOC ₁	0.38502	T _{1,1}
	0.38502	T _{1,-1}
	0.22741	T _{1,0}
	0.00094	T _{2,0}
	0.00018	T _{2,-1}
	0.00014	T _{9,-1}
	0.00018	T _{2,1}
	0.00014	T _{9,1}
	0.00012	S ₃
	0.00011	S ₁₂₀
SOC ₂	0.72031	T _{1,0}
	0.13860	T _{1,-1}
	0.13860	T _{1,1}
	0.00051	T _{2,1}
SOC ₃	0.00028	T _{2,0}
	0.00011	T _{7,-1}
	0.00011	T _{7,1}
	0.47442	T _{1,-1}
	0.47442	T _{1,1}
	0.04985	T _{1,0}
	0.00011	T _{7,0}
	0.00011	T _{9,0}
	0.00011	T _{7,-1}
	0.00011	T _{7,1}
	0.00010	T _{9,-1}
	0.00010	T _{9,1}

Table S4. k_r , ΔE_{1i} , and ρ_{298K} of each SOCn for (R_a, R_a)-anti-**1**.

	k_r [s]	ΔE_{1i} [cm ⁻¹]	ρ_{298K}
SOC ₁	4.4×10^2	-	0.333
SOC ₂	1.1×10^2	0.2	0.333
SOC ₃	4.7×10^3	2.1	0.331

Table S5. Cartesian coordinates of (R_a, R_a)-anti-**1** in the T₁ state.

atom	x	y	z				
C	-0.413774	0.428164	3.964999	C	6.395052	-1.9885	-1.760868
C	-0.818713	0.919553	5.217961	C	7.684966	-0.053811	0.350995
C	-0.361281	0.359342	6.408695	C	7.480168	-1.713126	2.082298
C	0.520894	-0.721026	6.366387	C	5.798431	-2.385088	-2.916031
C	0.952953	-1.207347	5.135078	C	3.439686	-2.923025	-3.571757
C	0.50971	-0.648964	3.922067	C	1.154511	-3.684921	-4.287692
C	0.50971	-0.648964	3.922067	C	-0.053722	-3.840986	-3.633199
H	-1.506129	1.760069	5.245745	C	-2.46766	-5.338235	-1.48749
H	-0.693064	0.764075	7.360963	C	-3.201193	-3.095252	-2.136763
H	0.875403	-1.180519	7.285019	H	7.44825	-1.838014	-1.57814
H	1.647066	-2.041521	5.097544	H	7.260735	0.502261	-0.479788
C	1.056255	-1.201726	2.641841	C	8.981356	0.245862	0.776613
C	2.461659	-1.038082	2.41279	C	8.770774	-1.435899	2.507039
C	0.183715	-1.889452	1.779673	H	6.900933	-2.476301	2.593139
N	3.139057	-1.451863	1.285454	H	6.26425	-2.618315	-3.864962
C	3.378459	-0.443276	3.320098	H	3.802005	-3.140642	-4.572246
N	0.475821	-2.331026	0.518741	H	1.391464	-3.917513	-5.317818
C	-1.172975	-2.264871	2.115532	H	-0.984317	-4.217217	-4.032572
C	4.469054	-1.141854	1.47908	C	-3.729936	-5.827731	-1.837319
Pt	2.297232	-2.221617	-0.419299	C	-1.412509	-6.280459	-0.951808
C	4.630916	-0.513502	2.738012	C	-2.945304	-1.613982	-2.304428
H	3.130548	-0.021314	4.282036	H	9.540135	1.022202	0.266607
C	-0.674119	-2.927737	0.016807	C	9.533535	-0.450781	1.858148
C	-1.696206	-2.901911	1.037582	H	9.215888	-1.97022	3.340525
H	-1.648312	-2.071672	3.064151	H	-3.931387	-6.890635	-1.716533
C	5.529913	-1.351984	0.530609	C	-4.734304	-4.992606	-2.337083
N	4.13414	-2.132585	-1.350369	H	-1.109595	-6.009846	0.066748
N	1.441816	-2.986284	-2.126425	H	-0.506416	-6.257663	-1.568563
H	5.560813	-0.140924	3.139707	H	-1.782702	-7.310161	-0.93125
C	-0.856571	-3.411778	-1.269613	H	-2.049842	-1.427338	-2.908164
H	-2.687757	-3.315688	0.924012	H	-2.786053	-1.113888	-1.341658
C	5.347334	-1.800359	-0.777414	H	-3.792056	-1.124583	-2.795393
C	6.910049	-1.034859	0.985405	O	10.78553	-0.248787	2.355641
C	4.384401	-2.487198	-2.650912	C	-6.078932	-5.553636	-2.739799
C	2.071089	-3.163391	-3.337441	C	11.60369	0.735661	1.743245
C	0.14383	-3.404896	-2.295416	H	-6.849298	-4.775358	-2.755629
C	-2.205023	-3.959647	-1.636362	H	-6.407315	-6.342142	-2.053116

H	-6.041699	-5.996181	-3.744406	C	3.074587	3.437015	-2.036519
H	12.5467	0.724925	2.292624	H	-7.445344	1.734153	-1.300921
H	11.154	1.734822	1.814193	H	-6.858152	-0.946138	-0.339072
H	11.79585	0.500743	0.688015	C	-8.664408	-0.917266	0.822759
C	-0.99456	1.054942	2.727936	C	-8.793338	0.814236	2.509808
C	-2.369131	0.873033	2.500479	H	-7.104288	2.127661	2.646496
C	-0.150851	1.806064	1.898415	H	-6.397121	2.973672	-3.455445
N	-3.083417	1.33104	1.413978	H	-3.998099	3.797911	-4.113597
C	-3.26689	0.16253	3.38192	H	-1.652972	4.743835	-4.817361
N	-0.487683	2.368489	0.687221	H	0.768999	4.867418	-3.624395
C	1.221635	2.133731	2.205434	C	3.661333	6.095506	-1.390643
C	-4.393934	0.935746	1.58612	C	1.396555	6.447403	-0.343135
Pt	-2.32357	2.328319	-0.194005	C	2.791028	1.99423	-2.391656
C	-4.505486	0.207058	2.825565	H	-9.080297	-1.773416	0.303855
H	-2.98172	-0.307256	4.311123	C	-9.36804	-0.285932	1.855138
C	0.639401	3.000777	0.205033	H	-9.35405	1.295258	3.305257
C	1.705771	2.863972	1.167878	H	3.886576	7.128778	-1.132677
H	1.741424	1.839966	3.103678	C	4.628533	5.327523	-2.04602
C	-5.459502	1.15091	0.699549	H	1.099346	6.017679	0.620672
N	-4.169512	2.295623	-1.07207	H	0.479195	6.562729	-0.932519
N	-1.556922	3.332481	-1.799882	H	1.805607	7.445362	-0.156866
H	-5.41852	-0.225827	3.206216	H	1.893834	1.900599	-3.014341
C	0.770802	3.651765	-1.026775	H	2.619231	1.380143	-1.499621
H	2.697056	3.276611	1.049043	H	3.630113	1.555779	-2.940644
C	-5.334159	1.788179	-0.54121	O	-10.60439	-0.658917	2.295793
C	-6.813898	0.652331	1.099461	C	5.963583	5.923583	-2.429933
C	-4.482886	2.821119	-2.303345	C	-11.23502	-1.764656	1.67083
C	-2.24721	3.682858	-2.936155	H	6.736116	5.15224	-2.519346
C	-0.265811	3.781234	-1.958205	H	6.302315	6.658884	-1.691547
C	2.112315	4.233589	-1.380119	H	5.906502	6.440286	-3.397683
C	-6.417488	2.01758	-1.47222	H	-12.19792	-1.882811	2.171253
C	-7.400742	-0.44389	0.457221	H	-10.64903	-2.685655	1.79113
C	-7.53649	1.271929	2.135239	H	-11.40293	-1.582722	0.60085
C	-5.889193	2.643327	-2.558317	C	-4.449026	-3.632001	-2.476426
C	-3.594765	3.445859	-3.168877	H	-5.216127	-2.96407	-2.864116
C	-1.361737	4.36403	-3.846367	C	4.315206	4.001528	-2.356194
C	-0.142597	4.427566	-3.246052	H	5.055554	3.384199	-2.861721
C	2.407695	5.574419	-1.053312				

